

Genetic interaction of *Gli3* and *Alx4* during limb development

LIA PANMAN^{*,a}, THIJS DRENTH^b, PASCAL TEWELSCHER^c, AIMÉE ZUNIGA¹ and ROLF ZELLER¹

Department of Developmental Biology, Utrecht University, Utrecht, The Netherlands and ¹Developmental Genetics, DKBW Centre for Biomedicine, University of Basel Medical School, Basel, Switzerland.

ABSTRACT The *Gli3* and *Alx4* transcriptional regulators are expressed in the anterior limb bud mesenchyme and their disruption in mice results in preaxial polydactyly. While the polydactylous phenotype of *Alx4* deficient limb buds depends on SHH, the one of *Gli3* deficient limb buds is completely independent of SHH signalling, suggesting that these genes act in parallel pathways. Analysis of limb buds lacking both *Gli3* and *Alx4* now shows that these two genes interact during limb skeletal morphogenesis. In addition to the defects in single mutants, the stylopod is severely malformed and the anterior element of the zeugopod is lost in double mutant limbs. However, limb bud patterning in *Gli3*^{-/-}; *Alx4*^{-/-} double mutant embryos is not affected more than in single mutants as the expression domains of key regulators remain the same. Most interestingly, the loss of the severe preaxial polydactyly characteristic of *Gli3*^{-/-} limbs in double mutant embryos establishes that this type of polydactyly requires *Alx4* function.

KEY WORDS: *Hox* gene, limb development, preaxial polydactyly, radius, SHH, tibia

The semi-dominant mouse mutations *Extra-toes* (*Xt*) and *Strong's Luxoid* (*Lst*), are loss-of-function mutations disrupting the zinc-finger encoding transcription factor *Gli3* (Schimmang *et al.*, 1992; Hui and Joyner, 1993) and the *aristaless*-related homeobox gene *Alx4* (Qu *et al.*, 1998; Takahashi *et al.*, 1998), respectively. In the homozygous state, both mouse mutations cause pleiotropic and lethal congenital malformations with distinct preaxial limb polydactylies. In both mutants, an anterior ectopic *Sonic Hedgehog* (SHH) signalling centre is established in addition to the one in the posterior limb bud mesenchyme (Masuya *et al.*, 1995; Buscher *et al.*, 1997; Qu *et al.*, 1997). SHH is a morphogen produced by the polarizing region (or ZPA) in the posterior limb bud and is essential for controlling antero-posterior patterning of the limb skeleton (zeugopod and autopod; reviewed by Zeller, 2004). Only one anterior zeugopodal element and digit develop in limbs of embryos lacking SHH function (Chiang *et al.* 2001; Kraus *et al.*, 2001). Interestingly, the polydactylous phenotypes caused by the mutations in *Gli3* and *Alx4* differ with respect to their dependence on SHH signalling. The polydactyly of *Gli3* deficient limbs is SHH independent as limbs lacking both *Gli3* and *Shh* display a polydactyly identical to *Gli3* single mutants. In contrast, the one caused by disrupting *Alx4* is SHH dependent as only one digit

forms in limbs lacking both *Alx4* and *Shh* (for details see te Welscher *et al.*, 2002b). Indeed, *Gli3* functions first in a mutually antagonistic interaction with *dHand*, which seems to pre-pattern the limb bud mesenchyme already prior to *Shh* activation (te Welscher *et al.*, 2002a). In contrast, *Alx4* does not seem to function during this early determinative phase upstream of SHH mediated limb bud patterning. Additional striking differences between the two mutant limb phenotypes (Qu *et al.*, 1997; Zuniga *et al.*, 1999; te Welscher *et al.*, 2002b) are a likely consequence of their differential functions: anterior expansion of the normally posteriorly restricted expression domains of *Gremlin* and *5'Hoxd* genes is apparent from the earliest limb bud stages onwards in *Gli3* deficient limb buds. In contrast, small anterior ectopic expression domains appear only much later in *Alx4* deficient limb buds. Furthermore, *Alx4* expression is reduced in *Gli3* deficient limb buds, indicating that *Gli3* acts genetically upstream of *Alx4* (te Welscher *et al.*, 2002a). However, the remaining, more proximally restricted *Alx4* expression in *Gli3*^{-/-} mutant limb buds also indicates that *Alx4* may function at least in part independent of *Gli3*. Taken together, these and other studies establish that *Gli3*, but not

Abbreviations used in this paper: *Xt*, extra toes.

a) Present address: Ludwig Institute for Cancer Research, Department of Cell and Molecular Biology, Karolinska Institute, Box 240, S-17177 Stockholm, Sweden.

b) Present address: INSERM U.623-IBDM, Campus de Luminy-Case 907, F-13288 Marseille Cedex 09, France.

c) Present address: EMBL Monterotondo, Mouse Biology Unit, Via Ramarini 32, 00016 Monterotondo, Italy.

*Address correspondence to: Dr. Lia Panman. Ludwig Institute for Cancer Research, Department of Cell and Molecular Biology, Karolinska Institute, Box 240, S-17177 Stockholm, Sweden. Fax: +46-8-332-812. e-mail: lia.panman@licr.ki.se

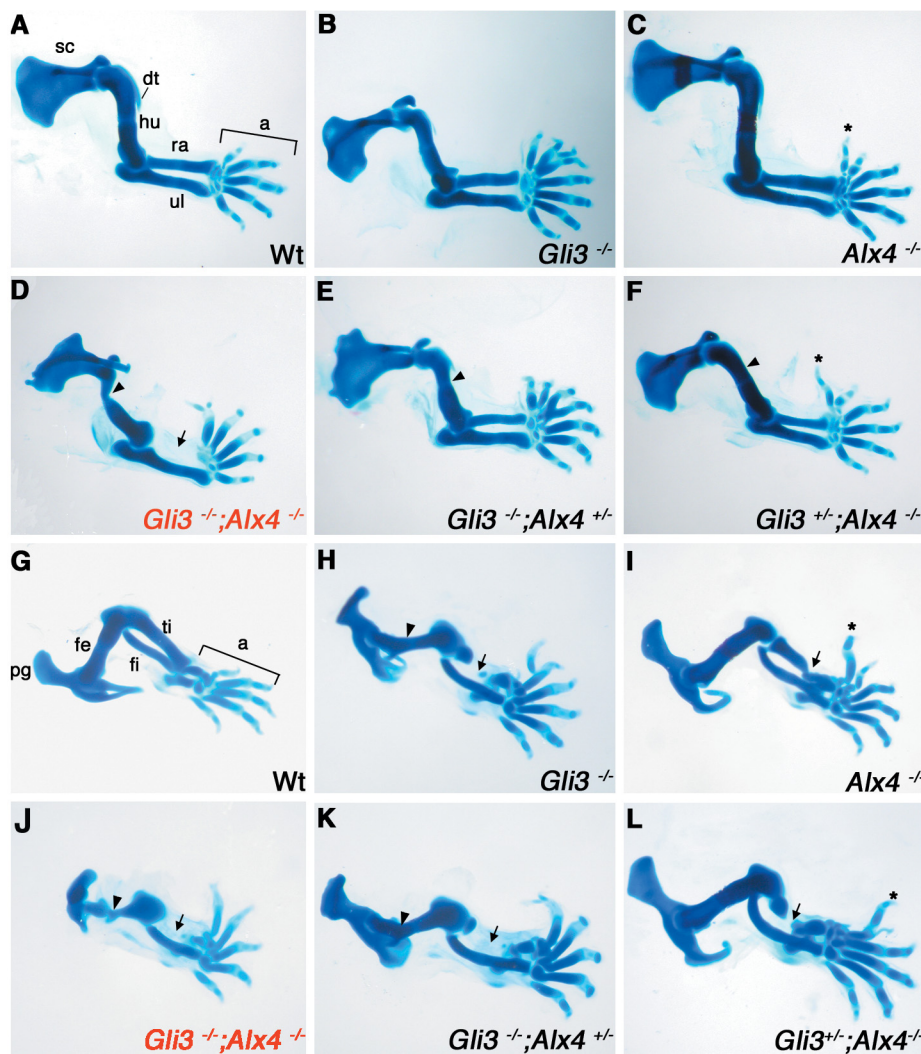


Fig. 1. Skeletal preparations of limbs of single and compound mutant embryos lacking *Gli3* and/or *Alx4* at gestational day E14.5. (A-F) forelimbs, (G-L) hindlimbs, cartilage appears blue as stained by alcian blue. As ossification is just being initiated, none or only few ossification centres become apparent as darker areas (alizarin red). (A) Wild-type forelimb. (B) *Gli3*^{-/-} homozygous forelimb. Note the preaxial polydactyly and loss of digit identity. (C) *Alx4*^{-/-} homozygous forelimb. Asterisk indicates a duplicated preaxial digit 2. (D) *Gli3*^{-/-}; *Alx4*^{-/-} double homozygous forelimb. Arrowhead points to the malformed humerus. Arrow points to the anterior zeugopodal region lacking the radius. Note the duplication of the distal phalange of the most anterior digit. (E) *Gli3*^{-/-}; *Alx4*^{+/-} mutant forelimb, arrowhead indicates the malformed humerus. The preaxial polydactyly of the autopod is similar to the one of a forelimb lacking *Gli3* alone. (F) *Gli3*^{+/-}; *Alx4*^{-/-} mutant forelimb. Asterisk indicates the duplicated preaxial digit 2. Arrowhead points to the humerus lacking the deltoid tuberosity. Note that the phenotype of the autopod is identical to the one of a forelimb lacking *Alx4* alone. (G) Wild-type hindlimb. (H) *Gli3*^{-/-} homozygous hindlimb. Arrow points to the rudimentary tibia. (I) *Alx4*^{-/-} homozygous hindlimb. Arrow points to the deformed tibia. Asterisk indicates the duplicated preaxial digit 2. (J) *Gli3*^{-/-}; *Alx4*^{-/-} double homozygous hindlimb. Arrow points to the region lacking the tibia. Arrowhead indicates the malformed femur. (K) *Gli3*^{-/-}; *Alx4*^{+/-} mutant hindlimb. The femur (arrowhead) and tibia (arrow) are affected. (L) *Gli3*^{+/-}; *Alx4*^{-/-} mutant hindlimb. Arrow points to the malformed tibia. Asterisk points to the duplicated preaxial digit 2. All panels are oriented with anterior to the top and distal to the right. a, autopod; dt, deltoid tuberosity; hu, humerus; ra, radius; sc, scapula; ul, ulna; fe, femur; fi, fibula; pg, pelvic girdle; ti, tibia.

Alx4, acts initially up-stream of SHH to polarise the nascent limb bud mesenchyme (Masuya *et al.*, 1995; Buscher *et al.*, 1997; te Welscher *et al.*, 2002a). Subsequently, SHH mediated inhibition of *Gli3* protein processing produces a *Gli3* repressor gradient that has been proposed as essential to antero-posterior limb bud patterning (Wang *et al.*, 2000). During progression of limb bud development, *Alx4* becomes critical to suppress anterior ectopic *Shh* expression (Qu *et al.*, 1997). To uncover possible genetic interactions of *Gli3* and *Alx4*, we have generated *Gli3* and *Alx4* compound mutant embryos for analysis. Up to gestational day 14.5 (E14.5), all genotypes are recovered from litters at expected ratios (Fig. 1 and data not shown), but by E16.5 no double homozygous embryos

could be collected due to embryonic lethality (data not shown). The skeletons of four embryos lacking both *Gli3* and *Alx4* at E14.5 were analysed and all double homozygous limbs display skeletal defects that are distinct from the ones of all other genotypes (Fig. 1, 2 and data not shown; for summary see Table 1). In addition, severe craniofacial clefting of the nose region affects these embryos by E14.5 (data not shown).

Skeletal Phenotypes of Forelimbs

The scapula and stylopod of *Gli3*^{-/-}; *Alx4*^{-/-} double homozygous forelimbs are malformed (Fig. 1D; arrowhead points to malformed humerus) and the latter lacks a well-formed deltoid tuberosity. In contrast, the humerus of *Gli3* (Fig. 1B) and *Alx4* (Fig. 1C) single mutant embryos appears normal, while additional inactivation of either one *Gli3* or *Alx4* allele causes slight malformation of the humerus (arrowheads Fig. 1E, F). These results are indicative of a dose-dependent requirement of these two genes during humerus morphogenesis. In contrast to all other genetic combinations (Fig. 1A-C, 1E, F and data not shown), the zeugopod of *Gli3*^{-/-}; *Alx4*^{-/-} double homozygous forelimbs

TABLE 1

SKELETAL PHENOTYPES

	<i>Gli3</i> ^{-/-}	<i>Alx4</i> ^{-/-}	<i>Gli3</i> ^{-/-} ; <i>Alx4</i> ^{+/-}	<i>Gli3</i> ^{+/-} ; <i>Alx4</i> ^{-/-}	<i>Gli3</i> ^{-/-} ; <i>Alx4</i> ^{-/-}
Humerus	wild-type	wild-type	slightly abnormal	slightly-abnormal	malformed
Radius	wild-type	wild-type	wild-type	wild-type	complete aplasia
Femur	slightly abnormal	wild-type	slightly abnormal	wild-type	malformed
Tibia	malformed	malformed	complete aplasia	malformed	complete aplasia
Digit number	~ 8	6	~ 7	6	5 (6)

lacks the radius (arrow, Fig. 1D), while the ulna forms correctly. Finally, the autopod of double homozygous limbs is distinct from all other mutant combinations (Fig. 1D and Fig. 2A-F, for details see below).

Skeletal Phenotypes of Hindlimbs

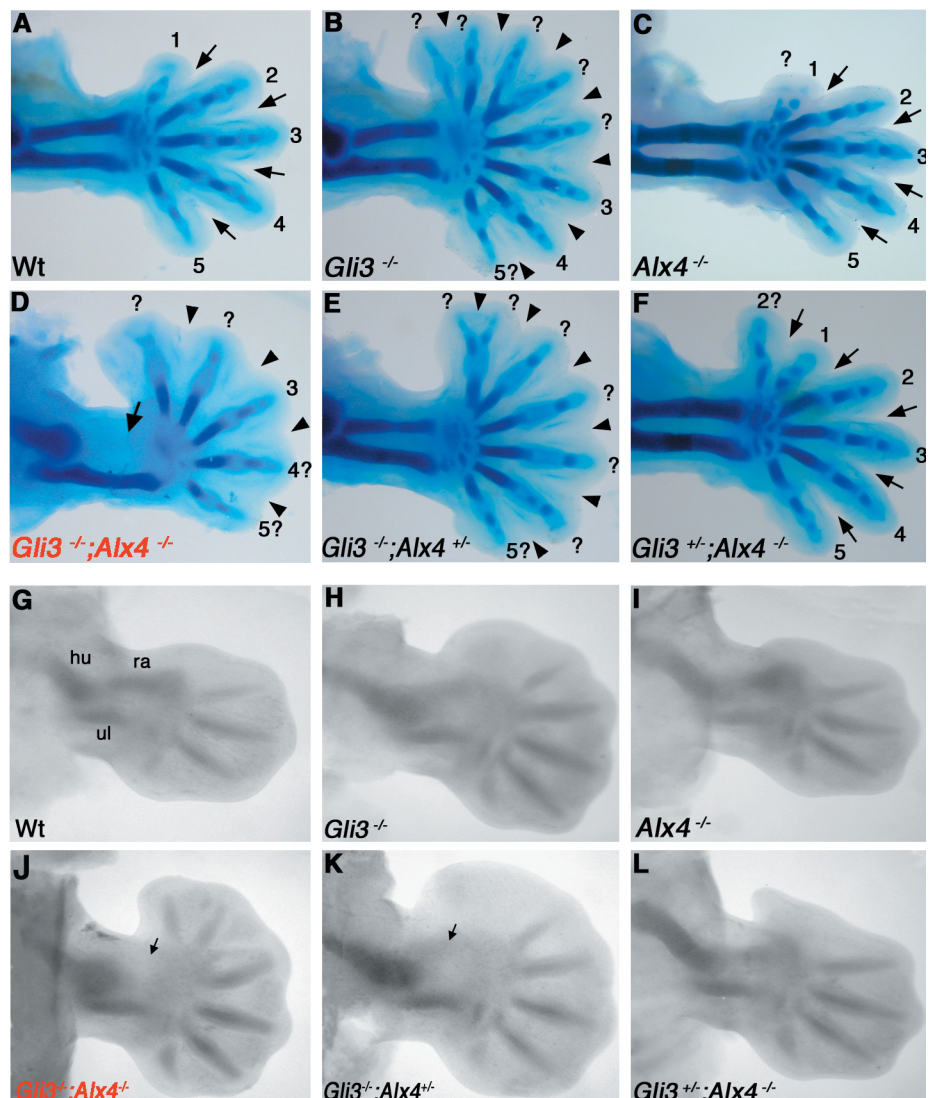
Similar to the forelimbs, the pelvic girdle and femur of *Gli3*^{-/-}; *Alx4*^{-/-} double homozygous hindlimbs are severely malformed (arrowhead, Fig. 1J). The femur of *Gli3*^{-/-}; *Alx4*^{+/-} compound mutant hindlimbs (arrowhead Fig. 1K) is affected similar to *Gli3*^{-/-} limbs (arrowhead in Fig. 1H), while it is normal in embryos lacking *Alx4* (Fig. 1I, L). In contrast to forelimbs, the tibia is missing in both *Gli3*^{-/-}; *Alx4*^{-/-} and *Gli3*^{-/-}; *Alx4*^{+/-} limbs (arrows in Figs. 1J, K) and its medial part is deleted in *Gli3*^{-/-} single (arrow, Fig. 1H) and *Gli3*^{+/-}; *Alx4*^{-/-} compound mutant hindlimbs (arrow, Fig. 1L). Furthermore, the tibia is also deformed in *Alx4*^{-/-} single mutant embryos (Fig. 1I), which shows that both genes are required and apparently fulfil only partially overlapping functions during tibia morphogenesis. Development of the hindlimb autopod (Fig. 1G-L) is affected similarly to forelimbs.

Phenotypes of the Autopod

An additional preaxial digit forms in *Alx4*^{-/-} limbs (Fig. 1C, 2C) in comparison to wild-type limbs (Fig. 1A, 2A), irrespective of the presence of either both (Fig. 1C, 2C; see also Qu *et al.* 1997) or only one functional *Gli3* allele (Fig. 1F, 2F). In contrast, the autopods of *Gli3* deficient limbs display severe preaxial polydactylies with up to eight digits (Fig. 1B, 2B). In agreement with the

conclusions of recent studies (Ahn and Joyner, 2004; Harfe *et al.*, 2004), the posterior 3 digits retain distinct identities, while the five anterior-most digits lack defined identity (as indicated by question marks in Fig. 2B). Rather unexpectedly, complete inactivation of *Alx4* and *Gli3* (Fig. 1D and Fig. 2D) reduces digit numbers from eight (Fig. 2B, E) to five or six (Fig. 1D, 2D, 2J). The posterior three digits retain at least partial posterior identities (similar to *Gli3*^{-/-}; compare Fig. 2D to 2B), while the anterior two digits display no defined identities. Most importantly, these results establish that the severe preaxial polydactylous limb phenotype of *Gli3* deficient embryos (Fig. 1B, 2B) depends on *Alx4* function. While digits 2 to 5 are patterned under the influence of SHH-mediated graded inhibition of *Gli3* repressor formation, the most anterior digit 1 and the anterior zeugopod (radius and tibia) are specified by a so far unknown other mechanism (reviewed by Zeller, 2004). The results of our study now suggest that interaction of the *Alx4* transcription factor with the *Gli3* (repressor) protein may be involved in specifying the anterior-most limb skeletal elements (digit 1, radius and tibia). In support of this proposal, the characteristic duplicated preaxial digit observed in forelimbs lacking *Alx4* but not *Gli3* (Fig.

Fig. 2. Skeletal phenotypes forelimbs of different genotypes at E14.5 and E12.5. (A-F) forelimbs at gestational day E14.5. (A) Wild-type control. (B) *Gli3* deficient forelimb. Note the preaxial polydactyly, loss of anterior identities and webbing. (C) *Alx4* deficient forelimb. Note the additional preaxial digit. (D) *Gli3*^{-/-}; *Alx4*^{-/-} forelimb. Note the lack of the radius (arrow), duplicated of the distal phalange of the most anterior digit and general webbing. (E) *Gli3*^{-/-}; *Alx4*^{+/-} forelimb. Note the preaxial polydactyly and webbing similar to *Gli3*^{-/-} forelimbs. (F) *Gli3*^{+/-}; *Alx4*^{-/-} forelimb. Note the additional preaxial digit. Arrows in (A), (C) and (F) indicate the interdigital areas separating the digits through apoptosis. Arrowheads in (B), (D) and (E) indicate webbing in forelimbs of embryos lacking *Gli3*. Digits are numbered according to their apparent identities. Question marks indicate unclear identities. (G-L) Alcian green staining of the forming cartilage elements in forelimbs at E12.5. (G-I, L) The cartilage primordia of the radius has formed in (G) wild-type, (H) *Gli3*^{-/-}, (I) *Alx4*^{-/-} and (L) *Gli3*^{+/-}; *Alx4*^{-/-} mutant forelimbs. (K) The radius primordia is only weakly apparent in *Gli3*^{-/-}; *Alx4*^{+/-} mutant forelimbs (arrow). (J) The radius primordia is lacking in *Gli3*^{-/-}; *Alx4*^{-/-} double mutant forelimbs (arrow). All forelimbs are oriented with anterior to the top and distal to the right. hu, humerus; ra, radius; ul, ulna.



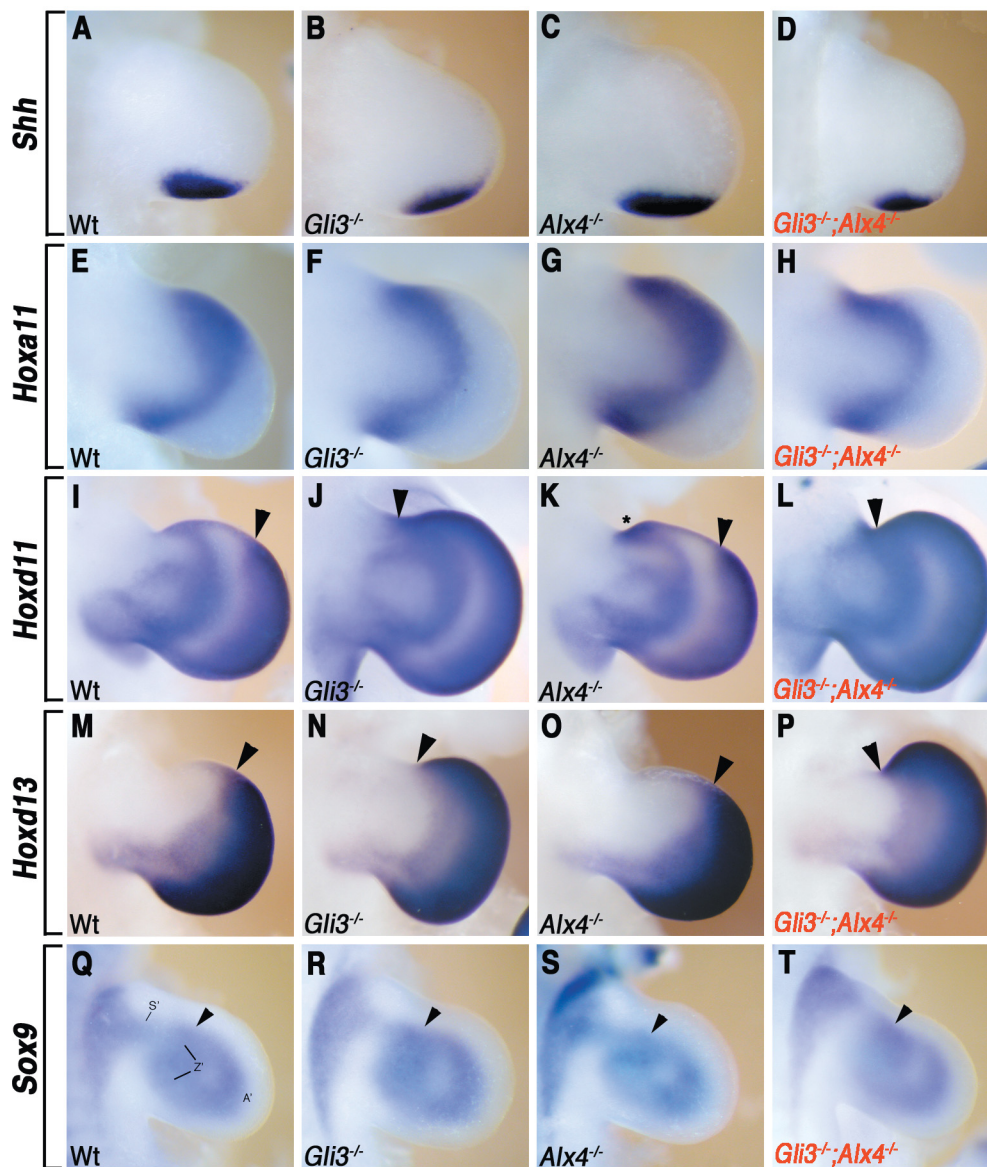


Fig. 3. Molecular analysis of key regulators of limb bud patterning. (A-D) *Shh* expression in wild-type and mutant forelimb buds (E10.75). At this stage, there are no significant differences in *Shh* expression between wild-type (A), single (B,C) and double homozygous mutant limb buds (D). Anterior ectopic *Shh* expression is detected much later in mutant limb buds (data not shown; Buscher et al., 1997; Masuya et al., 1995; Qu et al., 1997). (E-H) Expression of *Hoxa11* in wild-type and mutant forelimb buds (E11.5). Note that the *Hoxa11* expression domain in *Gli3*^{-/-}; *Alx4*^{-/-} limb buds (H) is identical to the one in *Gli3*^{-/-} limb buds (F). (I-L) *Hoxd11* expression in wild-type and mutant forelimb buds (E11.75). Again the *Hoxd11* expression domain in *Gli3*^{-/-}; *Alx4*^{-/-} (L) and *Gli3*^{-/-} limb buds (J) are similar. (M-P) *Hoxd13* expression in the distal limb mesenchyme of wild-type and mutant limb buds (E11.75). The *Hoxd13* expression in *Gli3*^{-/-}; *Alx4*^{-/-} limb buds (P) again resembles the one of *Gli3*^{-/-} limb buds (N). Arrowheads in (I-P) indicate the anterior boundaries of the distal (autopod) expression domains. Asterisk in (K) indicates the ectopic anterior domain of *Hoxd11* expression (Qu et al., 1997). (Q-T) *Sox9* expression in wt and mutant limb buds (E11). *Sox9* marks pre-cartilaginous condensations of mesenchymal cells. No significant differences are apparent. Arrowheads point to the approximate position of the condensation giving rise to the primordia of the radius. S': prospective stylopod; Z': prospective zeugopod; A': prospective autopod. All limb buds are oriented with anterior to the top and distal to the right.

1C, F and Fig. 2C, F) is also absent in most double mutant forelimbs (Fig. 1D, 2D). However, the distal most phalange of the most anterior digit is often duplicated (Fig. 1D, 2D). In contrast to inactivation of both *Alx4* alleles (arrows, Fig. 2C, F), the loss of *Gli3* functions causes interdigital webbing (arrowheads, Fig. 2B, E) by blocking interdigital apoptosis (Macias et al., 1999). This interdigital webbing is not altered by concurrent removal of *Alx4* in double homozygous limbs (Fig. 2D), which points to a non-redundant and essential function of *Gli3* in interdigital apoptosis.

Phenotypes of the Zeugopod

The most severe additional limb skeletal defect observed in embryos lacking both *Gli3* and *Alx4* in comparison to single homozygous mutants is the loss of the anterior zeugopodal element (radius and tibia, Fig. 1). Analysis of advanced limb bud patterning stages (E12.5, Fig. 2G-L) shows that the cartilage model giving rise to the radius does not form in double homozygous limb buds (arrow, Fig. 2J). Unexpected from the analysis of

older stages (Fig. 1E, 2E), the radius primordia is also less prominent in *Gli3*^{-/-}; *Alx4*^{-/-} compound mutant limb buds at this stage (arrow, Fig. 2K) than in wild-type (Fig. 2G) and the other genotypes (Fig. 2H, I, L and data not shown). These results indicate that formation of the radius is delayed in limbs lacking *Gli3* and one copy of *Alx4* (Fig. 2K), but catches up during its subsequent development (Fig. 1E, 2E) in contrast to the resulting aplasia in double homozygous forelimbs (Fig. 1D, 2D, 2J).

Normal Expression of Molecular Markers of Limb Bud Patterning

As in particular formation of anterior skeletal elements is disrupted in double homozygous limbs, the expression of relevant key regulators was analysed. *Shh* remains expressed normally in the posterior mesenchyme of single and double homozygous limb buds (Fig. 3A-D). No precocious anterior ectopic *Shh* expression is observed in double homozygous limb buds (Fig. 3D) as is the case later in single mutant limb buds (Masuya et al., 1995; Buscher

et al., 1997; Qu *et al.*, 1997). Genetic analysis has established that the paralogous *Hoxa11* and *Hoxd11* genes interact to specify the ulna and radius (Davis *et al.*, 1995) and proximal miss-expression of *Hoxd13* inhibits zeugopod morphogenesis (Goff and Tabin, 1997). Therefore, these three *Hox* genes are good candidates to detect alterations affecting zeugopod patterning. However, expression and distribution of neither *Hoxa11* nor *Hoxd11* transcripts (Fig. 3H, L) is significantly altered in *Gli3*^{-/-}; *Alx4*^{-/-} double homozygous forelimb buds in comparison to *Gli3* deficient counterparts (Fig. 3F, 3J). Furthermore, no significant changes in *Hoxd13* expression are observed in *Gli3*^{-/-}; *Alx4*^{-/-} double homozygous limb buds (Fig. 3P) in comparison to single mutant and wild-type limb buds (Fig. 3M-O). Therefore, the absence of the radius is not paralleled by consistent changes in the expression patterns of these three *Hox* genes during stages of limb bud patterning. In particular, the anterior limits of the *Hoxd11* and *Hoxd13* expression domains in the distal limb bud mesenchyme of *Gli3*^{-/-}; *Alx4*^{-/-} embryos (arrowheads, Fig. 3L, P) are identical to the ones in *Gli3*^{-/-} limb buds (arrowheads, Fig. 3J, N) and differ significantly from the ones in *Alx4*^{-/-} and wild-type limb buds (arrowheads, Fig. 3I, K, M, O). These results indicate that *Gli3*, but not *Alx4*, is required to regulate the anterior limits of the *Hoxd11* and *Hoxd13* expression domains. The establishment of these expression domains is regulated by *Gli3* already during onset of limb bud development (Zuniga and Zeller, 1999). Finally, the *Sox9* transcription factor is expressed by the condensing mesenchymal cells that prefigure the limb cartilage elements (Wright *et al.*, 1995). Analysis of *Sox9* expression reveals that the mesenchymal condensations are induced apparently normal in *Gli3*^{-/-}; *Alx4*^{-/-} double homozygous limb buds (Fig. 3T; compare to Fig. 3Q-S). Taken together, the results shown in Figure 3 indicate that the patterning events directing initiation of mesenchymal condensations and cartilage models, in particular the anterior limb bud, occur to the same extent in *Gli3*^{-/-}; *Alx4*^{-/-} and *Gli3*^{-/-} limb buds.

The present study reveals overlapping functions of *Gli3* and *Alx4* in formation of the radius, while truncations (but not complete loss) of the tibia have also been previously reported for *Alx4*^{-/-} and *Gli3*^{-/-} single mutant limbs (Johnson, 1967; Qu *et al.*, 1998). In forelimb buds lacking both *Fgf4* and *Fgf8*, the skeletal progenitors forming the zeugopodal condensations are reduced, which most likely directly causes loss of the radius (Sun *et al.*, 2002). In contrast, the apparently normal *Sox9* distribution in *Gli3*^{-/-}; *Alx4*^{-/-} double mutant limb buds indicates that the skeletal progenitor population is not reduced and induction of the mesenchymal condensations occurs apparently normal. Defects affecting the zeugopod are also observed in a variety of other mouse mutations, in particular those affecting *5'Hoxd* and *5'Hoxa* genes (Zakany and Duboule, 1999). For example, the mouse mutation *Ulnaless* (*Ul*) affects *cis*-regulation of *5'Hoxd* genes (Spitz *et al.*, 2003). Ectopic proximal *Hoxd13* together with reduced *Hoxd11* expression causes severe reduction of both zeugopod skeletal elements in limbs of *Ul* mutants embryos (Herault *et al.*, 1997; Peichel *et al.*, 1997). Moreover, Chen *et al.* (2004) have established that the *Gli3* repressor interacts directly with *Hoxd* proteins to promote digit specification. Therefore, it is possible to assume that the specific genetic interaction of *Gli3* with *Alx4* impacts on limb bud morphogenesis at the level of *Hox* protein regulation and

function rather than their expression.

Experimental Procedures

Gli3^{+/-}; *Alx4*^{+/-} double heterozygous mice were inter-crossed to obtain *Gli3*^{-/-}; *Alx4*^{-/-} double mutant embryos. Embryos and mice were genotyped as described by te Welscher *et al.* (2002b). Day of vaginal plug detection was defined as embryonic day 0.5. Embryos of gestational days 10.5-11.75 were dissected in PBS, fixed in 4% paraformaldehyde and processed for whole-mount *in situ* hybridization using digoxigenin-labelled antisense riboprobes as described by Haramis *et al.* (1995). Embryos were age-matched by determining their somite number (variation ± 2 somites). To visualize cartilage, embryos of gestational day E12.5 were fixed 5% TCA and subsequently stained with alcian green to visualize the cartilage. Embryos were cleared in methyl salicylate. Embryos of gestational days older than E14.0 were stained for cartilage and bone using standard alcian blue and alizarin red staining (Zeller *et al.*, 1989). However, either no or only small ossification centres (red) were detected by E14.5 (Fig. 2, 3)

Acknowledgements

The authors are grateful to V. Portegijs and H. Goedemans for technical assistance and C. Mueller-Thompson for help in preparing the manuscript. We thank G. Martin for providing the *Sox9* probe and F. Meijlink for helpful discussions and support. This study was supported by the Swiss National Science Foundation (R.Z), the Dutch NWO (R.Z), KNAW (A.Z) and the Stichting Catharine van Tussenbroek (L.P).

References

- AHN, S and JOYNER, A. L. (2004). Dynamic changes in the response of cells to positive hedgehog signaling during mouse limb patterning. *Cell* 118: 505-516.
- BUSCHER, D., BOSSE, B., HEYMER, J. and RUTHER, U. (1997). Evidence for genetic control of Sonic hedgehog by *Gli3* in mouse limb development. *Mech Dev* 62: 175-82.
- CHEN, Y., KNEZEVIC, V., ERVIN, V., HUTSON, R., WARD, Y. and MACKEM, S. (2004). Direct interaction with *Hoxd* proteins reverses *Gli3*-repressor function to promote digit formation downstream of *Shh*. *Development* 131: 2339-47.
- CHIANG, C., LITINGTUNG, Y., HARRIS, M.P., SIMANDL, B.K., LI, Y., BEACHY, P.A. and FALLON, J.F. (2001). Manifestation of the limb prepattern: Limb development in the absence of Sonic Hedgehog function. *Dev. Biol.* 236: 421-435.
- DAVIS, A. P., WITTE, D. P., HSIEH-LI, H. M., POTTER, S. and CAPECCHI, M. (1995). Absence of radius and ulna in mice lacking *hoxa-11* and *hoxd-11*. *Nature* 375: 791-795.
- GOFF, D. J. and TABIN, C. J. (1997). Analysis of *Hoxd-13* and *Hoxd-11* misexpression in chick limb buds reveals that *Hox* genes affect both bone condensation and growth. *Development* 124: 627-636.
- HARAMIS, A. G., BROWN, J. M. and ZELLER, R. (1995). The limb deformity mutation disrupts the SHH/FGF-4 feedback loop and regulation of 5'*HoxD* genes during limb pattern formation. *Development* 121: 4237-4245.
- HARFE B.D., S. P. J., NISSIM S., TIAN H., MCMAHON A.P. and TABIN C.J. (2004). Evidence for an expansion-based temporal *Shh* gradient in specifying vertebrate digit identities. *Cell* 118: 517-528.
- HERAULT, Y., FRAUDEAU, N., ZAKANY, J. and DUBOULE, D. (1997). *Ulnaless* (*Ul*), a regulatory mutation inducing both loss-of-function and gain-of-function of posterior *Hoxd* genes. *Development* 124: 3493-500.
- HUI, C. and JOYNER, A. (1993). A mouse model of greig cephalopolysyndactyly syndrome: the extra-toesJ mutation contains an intragenic deletion of the *Gli3* gene. *Nat-Genet.* 3: 241-246.
- JOHNSON, D. R. (1967). *Extra-toes*: a new mutant gene causing multiple abnormalities in the mouse. *J. Embryol. exp. Morph.* 17: 543-581.
- KRAUS, P., FRAIDENRAICH, D. and LOOMIS, C. A. (2001). Some distal limb structures develop in mice lacking Sonic hedgehog signaling. *Mech Dev* 100: 45-58.

- MACIAS, D., GANAN, Y., RODRIGUEZ-LEON, J., MERINO, R. and HURLE, J. M. (1999). Regulation by members of the transforming growth factor beta superfamily of the digital and interdigital fates of the autopodial limb mesoderm. *Cell Tissue Res.* 296: 95-102.
- MASUYA, H., SAGAI, T., WAKANA, S., MORIWAKI, K. and SHIROISHI, T. (1995). A duplicated zone of polarizing activity in polydactylous mouse mutants. *Genes Dev* 9: 1645-53.
- PEICHEL, C. L., PRABHAKARAN, B. and VOGT, T. F. (1997). The mouse *Ulnaless* mutation deregulates posterior HoxD gene expression and alters appendicular patterning. *Development* 124: 3481-3492.
- QU, S., NISWENDER, K., JI, Q., VAN DER MEER, R., KEENY, D., MAGNUSON, M. A. and WISDOM, R. (1997). Polydactyly and ectopic ZPA formation in *Alx-4* mutant mice. *Development* 124: 3999-4008.
- QU, S., TUCKER, S. C., EHRLICH, J. S., LEVORSE, J. M., FLAHERTY, L. A., WISDOM, R. and VOGT, T. F. (1998). Mutations in mouse *Aristaless-like4* cause Strong's Luxoid polydactyly. *Development* 125: 2711-21.
- SCHIMMANG, T., LEMAISTRE, M., VORTKAMP, A. and RÜTHER, U. (1992). Expression of the zinc finger gene *Gli3* is affected in the morphogenetic mouse mutant extra-toes (Xt). *Development* 116: 799-804.
- SPITZ, F., GONZALEZ, F. and DUBOULE, D. (2003). A global control region defines a chromosomal regulatory landscape containing the HoxD cluster. *Cell* 113: 405-17.
- TAKAHASHI, M., TAMURA, K., BUESCHER, D., MASUYA, H., YONEI-TAMURA, S., MATSUMOTO, K., NAITOH-MATSUO, M., TAKEUCHI, J., OGURA, K., SHIROISHI, T. *et al.* (1998). The role of *Alx-4* in the establishment of anteroposterior polarity during vertebrate limb development. *Development* 125: 4417-4425.
- TE WELSCHER, P., FERNANDEZ-TERAN, M., ROS, M. A. and ZELLER, R. (2002a). Mutual genetic antagonism involving *GLI3* and *dHAND* prepatterns the vertebrate limb bud mesenchyme prior to SHH signaling. *Genes Dev* 16: 421-426.
- TE WELSCHER, P., ZUNIGA, A., KUIJPER, S., DRENTH, T., GOEDEMAN, H. J., MEIJLINK, F. and ZELLER, R. (2002b). Progression of Vertebrate Limb Development through SHH-Mediated Counteraction of *GLI3*. *Science* 298: 827-830.
- WANG, B., FALLON, J. F. and BEACHY, P. A. (2000). Hedgehog-Regulated Processing of *Gli3* Produces an Anterior/Posterior Repressor gradient in the Developing Vertebrate Limb. *Cell* 100: 423-434.
- WRIGHT, E., HARGRAVE, M. R., CHRISTIANSEN, J., COOPER, L., KUN, J., EVANS, T., GANGADHARAN, U., GREENFIELD, A. and KOOPMAN, P. (1995). The Sry-related gene *Sox9* is expressed during chondrogenesis in mouse embryos. *Nat Genet* 9: 15-20.
- ZAKANY, J. and DUBOULE, D. (1999). Hox genes in digit development and evolution. *Cell Tissue Res.* 296: 19-25.
- ZELLER, R. (2004). It takes time to make a pinky: unexpected insights into how SHH patterns vertebrate digits. *Sci STKE* 2004: 53.
- ZELLER, R., JACKSON-GRUSBY, L. and LEDER, P. (1989). The *limb deformity* gene is required for apical ectodermal ridge differentiation and anteroposterior limb pattern formation. *Genes and Dev.* 3: 1481-1492.
- ZUNIGA, A., HARAMIS, A. P., MCMAHON, A. P. and ZELLER, R. (1999). Signal relay by BMP antagonism controls the SHH/FGF4 feedback loop in vertebrate limb buds. *Nature* 401: 598-602.
- ZUNIGA, A. and ZELLER, R. (1999). *Gli3* (Xt) and formin (ld) participate in the positioning of the polarising region and control of posterior limb-bud identity. *Development* 126: 13-21.

Received: January 2005

Reviewed by Referees: February 2005

Modified by Authors and Accepted for Publication: March 2005